

CrystEngComm

Accepted Manuscript



This is an *Accepted Manuscript*, which has been through the Royal Society of Chemistry peer review process and has been accepted for publication.

Accepted Manuscripts are published online shortly after acceptance, before technical editing, formatting and proof reading. Using this free service, authors can make their results available to the community, in citable form, before we publish the edited article. We will replace this *Accepted Manuscript* with the edited and formatted *Advance Article* as soon as it is available.

You can find more information about *Accepted Manuscripts* in the [Information for Authors](#).

Please note that technical editing may introduce minor changes to the text and/or graphics, which may alter content. The journal's standard [Terms & Conditions](#) and the [Ethical guidelines](#) still apply. In no event shall the Royal Society of Chemistry be held responsible for any errors or omissions in this *Accepted Manuscript* or any consequences arising from the use of any information it contains.

ARTICLE

Reductive coordination replication of V₂O₅ sacrificial macrostructures into vanadium-based porous coordination polymers

Cite this: DOI: 10.1039/x0xx00000x

Julien Reboul,^a Kenji Yoshida,^b Shuhei Furukawa,^{a,*} and Susumu Kitagawa^{a,b,*}Received 00th January 2012,
Accepted 00th January 2012

DOI: 10.1039/x0xx00000x

www.rsc.org/

Vanadium-based porous coordination polymers (or metal-organic frameworks) possess both porous and electronic properties, which make these new materials appealing for applications in molecular separation, sensing and heterogeneous catalysis. Their integration into systems that fully exploit their intrinsic properties requires versatile methods allowing assembly of the PCP crystals into well-defined films, patterns, fibers or the formation of heterostructures. In this contribution, polycrystalline macrostructures and heterostructures made of [V(OH)ndc]_n (with ndc = 1,4-naphthalenedicarboxylate) PCP crystals were synthesized through a dissolution-recrystallization process, so-called coordination replication, where a pre-shaped V₂O₅ sacrificial phase was replaced by well-intergrown PCP crystals in the presence of H₂ndc as an organic linker and under reductive environment. In this process, V₂O₅ acts both as the metal source and as the template that provides the shape to the resulting mesoscopic polycrystalline architecture. The ascorbic acid, acting as reductive agent both promotes the dissolution of the sacrificial V₂O₅ phase and provides the V^{III} species required for the construction of the [V(OH)ndc]_n framework. Two-dimensional patterns were successfully synthesized by applying this procedure.

Introduction

Porous coordination polymers (PCPs), also named metal organic frameworks (MOFs) are crystalline, porous materials built up from the assembly of metal ions with multifunctional organic linkers.¹ Beside their remarkable surface areas, one interesting feature of PCPs is the possibility of designing their pore size, shape and chemical properties by the judicious selection of both the metal centers and the organic ligands. In this regard, the choice of vanadium species as metal centers results in series of PCPs that are of particular interest, owing to their redox activity. Indeed, vanadium-based PCPs possess a strong potential in adsorption-separation and heterogeneous catalysis.² However, as any PCP frameworks, the application of vanadium-based PCPs into systems that fully exploit their inherent performances requires their integration into hierarchical structures, patterns or composites.³ Recently, we reported an innovative procedure for the structuration of PCPs based on the combination of sol-gel chemistry or solid state chemistry and pseudomorphic replacement.⁴ In this method, so-called coordination replication, a pre-shaped sacrificial metal oxide is replaced by a thermodynamically more stable PCP framework in the presence of multitopic organic ligands. Because the sol-gel process allows for the easy manufacture of a large range of nano-/macroscale materials (particles, thin films, coatings, membranes, patterns) based on a variety of

metal oxides,⁵ coordination replication appears as a general and powerful strategy for the processing of PCPs, whenever the kinetics of the sacrificial metal oxide dissolution can be coupled with the kinetics of PCP crystallization. This method was recently applied for the synthesis of PCP-based hierarchical structures and composites obtained from shaped aluminum,^{4,6} zinc⁷ and copper oxides.⁸

Herein, we report the extension of the coordination replication process to the redox-rich vanadium chemistry and demonstrate the synthesis of the first macroscopic structures made of vanadium-based PCP crystals. Regarding the coordination replication process, vanadium oxides are particularly suitable candidates as sacrificial templates for two main reasons. First, sol-gel chemistry of vanadium pentoxide (V₂O₅) gels is well-established⁹ and a variety of vanadium oxide morphologies, such as V₂O₅ thin films, foam monoliths, nanowires or nanorods and inverted opal structures are nowadays accessible.¹⁰ Second, V₂O₅ possesses fascinating electrochemical properties, which might be exploited to synthesize new porous composite materials. Indeed, the partial replication of a sacrificial metal oxide template possessing electrochemical properties might result in the formation of heterostructures that combines the porous properties of PCPs and the intrinsic properties of the remaining sacrificial phase. Recently, this strategy was opportunely applied by Zhan et al. who created new sensors with a selective photoelectrochemical

response by transforming the surface of semiconducting ZnO nanorods into a ZIF-8 shell layer acting as size selective filter.^{7a}

In the previous report, we demonstrated the replication of alumina two-dimensional patterns, hierarchically porous macrostructures⁴ and nanofibers¹¹ under microwave conditions into analogous structures made of $[\text{Al}(\text{OH})\text{ndc}]_n$, a three dimensional framework containing one-dimensional channels built of infinite chains of corner-sharing $\text{AlO}_4(\mu_2\text{-OH})_2$ interconnected by naphthalene dicarboxylate ligand.⁴ These successful results prompted us to attempt the synthesis of the vanadium-based isostructural compound, under similar experimental conditions. Because the utilization of V_2O_5 as metal source for the synthesis of vanadium-based PCPs was never demonstrated so far, we first determined the proper synthesis conditions in order to obtain $[\text{V}(\text{OH})\text{ndc}]_n$ from simple commercial V_2O_5 powders. Notably, the addition of ascorbic acid as reducing agent was found to be critical for the successful conversion of V_2O_5 into $[\text{V}(\text{OH})\text{ndc}]_n$. The synthesis conditions were then adjusted to successfully replicate vanadium oxide two-dimensional patterns into the corresponding $[\text{V}(\text{OH})\text{ndc}]_n$ -based structures (Fig. 1).

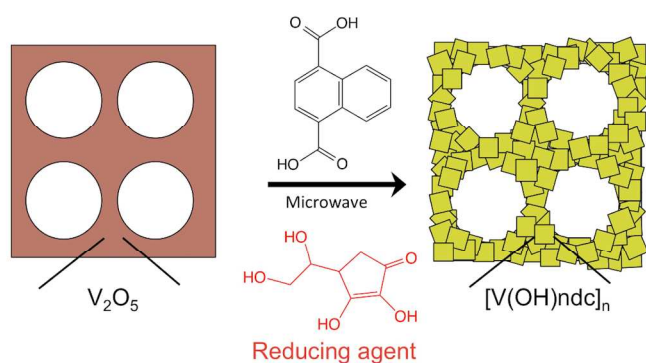


Fig. 1 Scheme of the replication of V_2O_5 sacrificial template into $[\text{V}(\text{OH})\text{ndc}]_n$ polycrystalline macrostructures.

Experimental Section

Materials

V_2O_5 (Wako, 99.0%), VCl_3 (Sigma-Aldrich, 97.0%), vanadium(V) oxytriisopropoxide (Sigma-Aldrich), 1,4-naphthalenedicarboxylic acid (H_2ndc , Wako, 95.0%), 1,4-benzenedicarboxylic acid (H_2bdc , Wako, 95.0%), polystyrene beads (PS, Polysciences, suspension in water, concentration = 2.6wt%), polyethylene oxide (PEO, 1000000 M_w , Sigma-Aldrich). All chemicals and solvents were purchased from commercial suppliers and used without further purification.

Syntheses of $[\text{V}(\text{OH})\text{ndc}]_n$ and $[\text{V}(\text{OH})\text{bdc}]_n$ from the V_2O_5 powder

Synthesis of $[\text{V}(\text{OH})\text{ndc}]_n$: 21.1 mg (0.116 mmol) of commercial V_2O_5 powders were mixed with 200 mg (0.925 mmol) of naphthalenedicarboxylic acid (H_2ndc) in 10 ml of water followed by the addition of 40.9 mg (0.232 mmol) of ascorbic acid to the mixture. The reaction mixture was then submitted to a microwave treatment for 10 min at 180°C. The green powder obtained at the end of the reaction was filtered and washed with distilled water and dimethylformamide (DMF).

Synthesis of $[\text{V}(\text{OH})\text{bdc}]_n$: 21.1 mg (0.11 mmol) of a commercial V_2O_5 powder was mixed with 154 mg (0.925 mmol) of H_2bdc in 5 ml of water. 40.9 mg (0.23 mmol) of ascorbic acid was then added to the mixture and the reaction mixture was submitted to a microwave treatment for 1 h at 180°C. The powder recovered after the thermal treatment was filtered and washed with distilled water and DMF. After the filtration and washing steps, the dried samples were treated at 250°C for 24h in air.

For comparison, $[\text{V}(\text{OH})\text{ndc}]_n$ and $[\text{V}(\text{OH})\text{bdc}]_n$ were also synthesized by following reported procedures using more conventional vanadium sources and hydrothermal treatments.¹²

Synthesis of $[\text{V}(\text{OH})\text{ndc}]_n$ from VCl_3 : a mixture of VCl_3 (157 mg, 1.00 mmol), H_2ndc (108 mg, 0.50 mmol), and H_2O (10 mL) was heated at 180 °C for 24 h under hydrothermal conditions. The powder recovered after the hydrothermal treatment was filtered and washed with distilled water.

Synthesis of $[\text{V}(\text{OH})\text{bdc}]_n$ from VCl_3 : a mixture of VCl_3 (841 mg, 5.35 mmol), H_2bdc (222 mg, 1.34 mmol), and H_2O (9.62 mL) was heated at 200 °C for 4 days under hydrothermal conditions. The powder recovered after the microwave treatment was filtered and washed with distilled water.

Syntheses of the vanadium oxide two-dimensional pattern

Two-dimensional pattern: an isopropanol solution of vanadium oxytriisopropoxide (0.22 mM) was drop-casted onto a two-dimensional assembly of polystyrene (PS) beads (diameter = 10 μm). The coating was then left in air and the partial hydrolysis takes place spontaneously due to ambient humidity. The negative structure of the PS bead assembly made of vanadium oxide was obtained after calcination of the PS beads at 250°C for 10h.

Replication of the patterns into the $[\text{V}(\text{OH})\text{ndc}]_n$ -based corresponding structure

Synthesis of the $[\text{V}(\text{OH})\text{ndc}]_n$ -based two-dimensional pattern: an ethanol solution of polyethylene oxide (PEO) (0.03 mM) was first spread onto the V_2O_5 pattern. After drying, the V_2O_5 pattern coated with PEO was placed into a water mixture (5 mL) of 1,4-naphthalenedicarboxylic acid (0.20 g ; 0.92 mmol) and ascorbic acid (0,08 g ; 0.45 mmol) and submitted to a microwave treatment at 180°C for 1 s (it necessarily takes one minute to reach 180 °C from room temperature). The sample recovered after the treatment was thoroughly washed with DMF and water.

Characterization

Field-emission scanning electron microscopy (FE-SEM) observations were performed with a JEOL Model JSM-75FCT FE-SEM system operating at 15 kV/20 μA . Dried samples were deposited on silicon wafer and coated with osmium prior to measurement. The CO_2 sorption isotherms of $[\text{V}(\text{O})(\text{ndc})]_n$ synthesized from V_2O_5 powder and VCl_3 were recorded at 195 K on a BELSORP-max volumetric-adsorption instrument from BEL Japan, Inc. All measurements were performed using the samples after pretreatment at 120 °C under vacuum conditions for 12 h. Powder X-ray Diffraction (XRD) data were collected on a Rigaku Model SmartLab equipped with a X-ray generator producing $\text{Cu K}\alpha$ radiation. Thermogravimetric (TG) analysis were performed using Rigaku Model Thermo Plus Evo II apparatus in the temperature range of 298-1023 K under nitrogen atmosphere, at a heating rate of 5 K min^{-1} . Fourier transform infrared (FT-IR) spectra were recorded either in

transmission mode (KBr pellets) or in the attenuated total reflectance mode (ATR) on a JASCO FT/IR-6100 spectrometer equipped with a TGS detector.

Results and discussion

[V(OH)ndc]_n synthesis from V₂O₅ powder

Prior to replication of V₂O₅ sacrificial templates into vanadium-based PCP macrostructures, we first established the experimental procedure to synthesize [V(OH)ndc]_n from a simple V₂O₅ powder under microwave conditions. Indeed, we previously demonstrated that microwave as heating source is necessary to efficiently replicate the details of the metal oxide sacrificial template. The integrity of the obtained product was verified by systematically comparing our results to that of the [V(OH)ndc]_n synthesized from VCl₃ under a more conventional solvothermal procedure. Synthesis from the V₂O₅ powder, in the presence of ascorbic acid as a reductant, results in a greenish powder that displays a similar X-ray diffraction (XRD) pattern to that made from VCl₃ after activation (250°C for 24h in air) (Fig. 2). The XRD patterns of these two activated materials match the calculated XRD pattern of [Al(OH)ndc]_n, hence verifying the structural analogy of these vanadium-based compounds with the aluminium-based framework first reported by Comotti et al.¹³ Compared to the XRD pattern of [Al(OH)ndc]_n, slight peak shifts towards lower values of 2θ were observed on the XRD pattern of the vanadium isostructural compounds. These shifts, also observed by Kozachuk et al., are supposedly due to the slight distortion of the [Al(OH)ndc]_n tetragonal symmetry when (Al^{III}OH)²⁺ sites are replaced by (V^{IV}O)²⁺ ones.

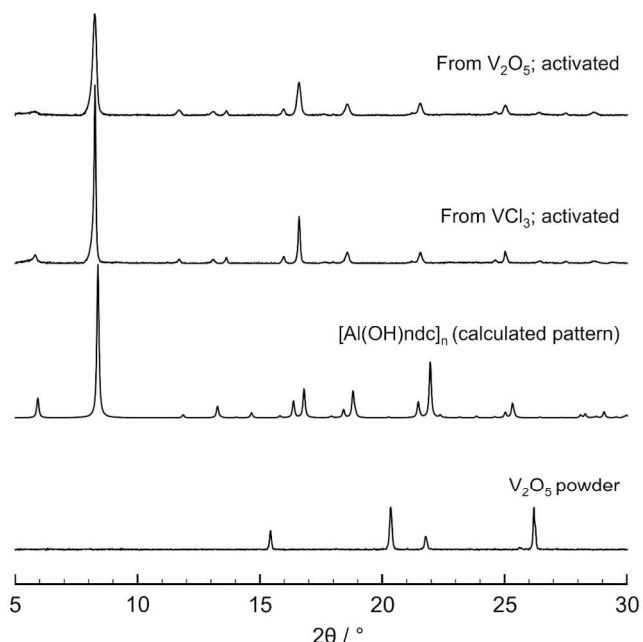


Fig. 2 XRD pattern of the activated [V(OH)ndc]_n obtained from V₂O₅ and from VCl₃, calculated pattern of [Al(OH)ndc]_n and XRD pattern of the commercial V₂O₅ powder.

As-synthesized products obtained from V₂O₅ and VCl₃ display similar infrared (IR) absorption patterns, which correspond to [V^{III}(OH)ndc]_n (Fig. 3). Similarly to the case of

the conventional synthesis from VCl₃, the activation of [V^{III}(OH)ndc]_n synthesized from V₂O₅ results in its transformation into [V^{IV}(O)ndc]_n, as evidenced by the total vanishing of the IR absorption band at 3640 cm⁻¹ assigned to the O-H vibrations of the μ₂-OH groups bridging the V^{III} centers within [V^{III}(OH)ndc]_n (Fig. 3). Note that in the case of the as-synthesized product obtained from V₂O₅, the band observed at 3640 cm⁻¹ is significantly weaker than that of the as-synthesized compound obtained from VCl₃ (Fig. 3, inset). This is likely due to the superior amount of species trapped within the pores of the as-synthesized [V^{III}(OH)ndc]_n obtained from V₂O₅ during the microwave treatment, as indicated by the larger weight loss up to 400°C observed on the TG trace corresponding to this product (Fig. S1). Indeed, Leclerc et al. demonstrated that H-bonded species (water molecules and unreacted ligands) incorporated within the pores during the synthesis of [V(OH)bdc]_n can disturb the OH group accessible along the inorganic chains and thereby results in the significant decrease of the bands at 3642 cm⁻¹.¹⁴ Higher amount of trapped species within the product obtained by microwave from V₂O₅ may be explained by the significantly higher nucleation and crystal growth rate allowed by microwave process.¹⁵ One should also consider the presence of the ascorbic acid within the reaction medium when using V₂O₅ as precursor. Indeed, owing to several hydroxyl groups in its composition, ascorbic acid may readily form hydrogen bonds with the OH groups accessible within [V(OH)ndc]_n pores under the synthesis conditions. It may therefore be easily trapped within the pores of the as-synthesized crystals and therefore affect the O-H vibrations. The oxidation of V^{III} into V^{IV} after activation was also evidenced by the development of the strong band observed at 910 cm⁻¹, which is attributed to the ν(V=O) mode of the asymmetric V-O-V bond sharing two consecutive VO₆ octahedra in [V^{IV}(O)ndc]_n (Fig. 3).¹⁶

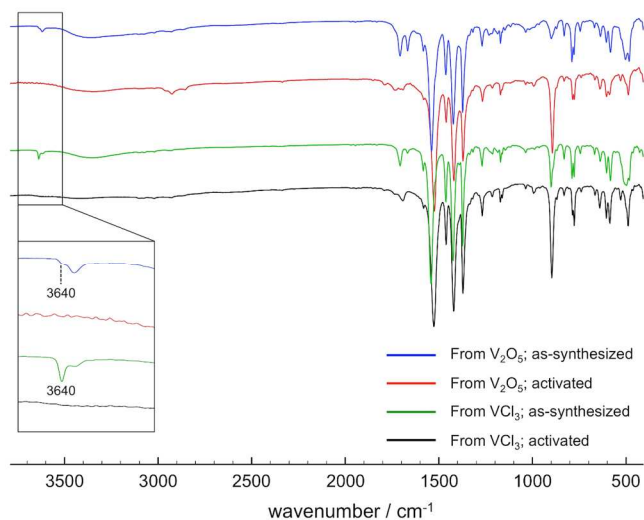


Fig. 3 IR spectra of [V(OH)ndc]_n before and after activation obtained from V₂O₅ and from VCl₃. The inset highlights the spectra region ranging from 3010 cm⁻¹ to 3750 cm⁻¹.

Raman analysis also clearly supported the formation of [V^{IV}(O)ndc]_n after activation with the development of the band attributed to ν(V=O) at 910 cm⁻¹ on the spectrum of the activated compounds (Fig. 4).¹⁴ Note that this band at 910 cm⁻¹ is actually already present on the Raman spectrum of the as-synthesized product, thus suggesting the presence of both [V^{III}(OH)]²⁺ and [V^{IV}(O)]²⁺ species within the framework even

before the activation process. The amplification of this band observed after activation, together with the total disappearance of the IR band at 3640 cm^{-1} (Fig. 3), evidences the complete oxidation of the V^{III} centers into V^{IV} . This result is in contrast to the previous reports about the synthesis of vanadium benzocarboxylate frameworks, in which only V^{III} centers were detected in the as-synthesized products.^{14,17} Since the Raman band at 910 cm^{-1} is also observed on the spectrum of the as-synthesized product obtained from VCl_3 , this particular feature may not be attributed to the use of V_2O_5 as vanadium source. We rather assume the spontaneous oxidation of V^{III} under ambient atmosphere during the storage and characterization of our as-synthesized product. This feature will not be further discussed here and the as-synthesized product will be designated as $[\text{V}^{\text{III}}(\text{OH})\text{ndc}]_n$ in the following.

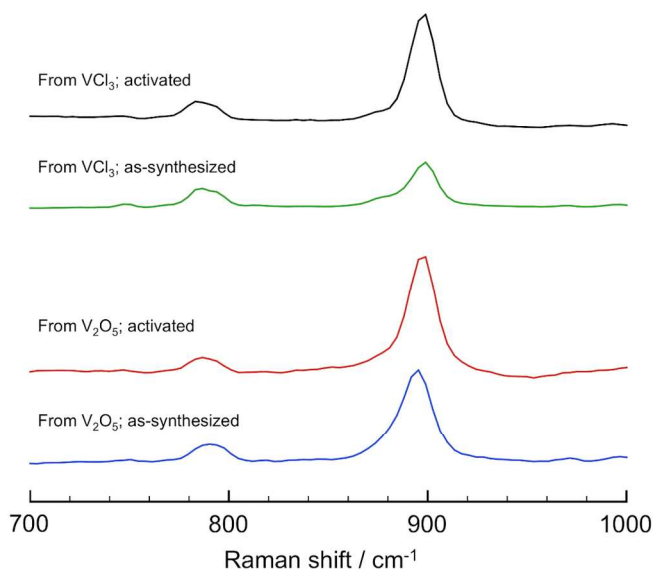


Fig. 4 Raman spectra of $[\text{V}(\text{OH})\text{ndc}]_n$ obtained from V_2O_5 and from VCl_3 before and after activation.

Thus, the strong similarity of the XRD patterns, IR and Raman spectra of the compounds obtained from V_2O_5 and VCl_3 supports the idea that the use of V_2O_5 as metal source results in the formation of equivalent $[\text{V}(\text{OH})\text{ndc}]_n$ crystals to that synthesized from VCl_3 , both in terms of crystal structure and chemical composition. Accordingly, no trace of unconverted V_2O_5 parent phase was detected by the characterization techniques employed in this study. Indeed, no diffraction peaks corresponding to unreacted V_2O_5 crystals were detected in the XRD pattern of $[\text{V}^{\text{IV}}(\text{O})\text{ndc}]_n$ synthesized from V_2O_5 (Fig. 2). The total conversion of V_2O_5 was also confirmed by the absence on the FT-IR spectra of the characteristic bands at 1011 cm^{-1} and 830 cm^{-1} commonly assigned to the stretching vibration of $\text{V}=\text{O}$ and asymmetric stretching of the $\text{V}-\text{O}-\text{V}$ bonds of crystalline V_2O_5 , respectively (Fig. 3).¹⁸ Furthermore, TG analysis of the activated $[\text{V}(\text{O})\text{ndc}]_n$ synthesized from VCl_3 and V_2O_5 confirmed that both compounds possess rigorously the same chemical composition. Indeed, TG traces of the two activated compounds display the same weight loss of 51.5% starting from approximately 270°C and corresponding to the degradation of the organic linkers (Fig. 5).

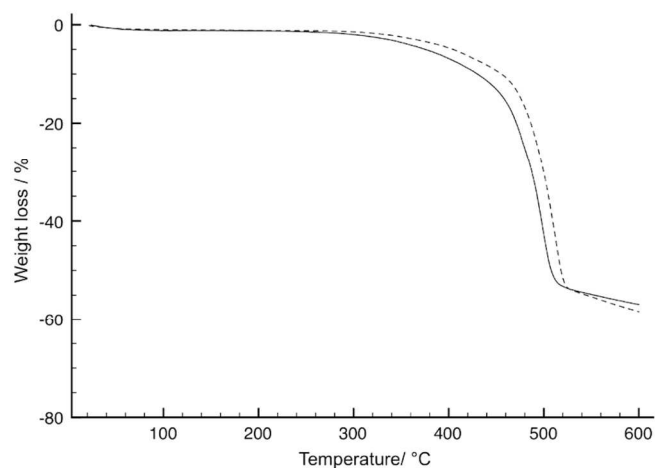


Fig. 5 Thermogravimetric analysis of $[\text{V}(\text{O})\text{ndc}]_n$ synthesized from V_2O_5 powder (solid line) and of $[\text{V}(\text{O})\text{ndc}]_n$ synthesized from VCl_3 (dash line).

Interestingly, field-emission scanning electron microscopy (FE-SEM) images shown in Fig. 6 indicate that the synthesis of $[\text{V}^{\text{IV}}(\text{O})\text{ndc}]_n$ from V_2O_5 under microwave irradiation results in crystals with smaller and more uniform size and shape than that synthesized from VCl_3 . Indeed, rod shaped crystals with length of 100 nm and width of 20 nm were obtained from V_2O_5 under microwave irradiation, while ill-defined crystals with size ranging from 100 nm to $1\text{ }\mu\text{m}$ were obtained under conventional synthesis conditions using VCl_3 . The smaller size of the crystals synthesized from V_2O_5 compared to that synthesized from VCl_3 may be responsible for the slightly wider X-ray diffraction peaks observed on the XRD pattern (Fig. 2) and for the rather lower decomposition temperature pointed out by the TG analysis (Fig. 5). In our previous study related to the conversion of Al_2O_3 phases into Al-based PCP crystals under microwave irradiation,⁴ a SEM time course analysis of the alumina sacrificial phase at the first stage of the PCP crystal formation revealed the fast formation of a very high amount of PCP nuclei covering the entire surface of the dissolving mineral precursor. Similarly, in the case of the synthesis of vanadium-based PCP, the combination of microwave irradiation and utilization of metal oxide as metal precursor may result in the formation of a higher number of PCP nuclei, and therefore in a higher number of smaller crystals than when VCl_3 precursor is used under conventional hydrothermal conditions. Noteworthy, the nanoscale and uniform size of the PCP crystals is a requirement for the successful replication of metal oxide structures by the coordination replication. Here this feature was exploited for the replication of the V_2O_5 pattern as shown below. CO_2 sorption analysis were performed with the $[\text{V}(\text{O})\text{ndc}]_n$ crystals obtained from both V_2O_5 and VCl_3 . The relatively small CO_2 adsorption amount on the sample from V_2O_5 , compared to the sample made from VCl_3 , might be related to a small amount of remaining ascorbic acid, which can easily block the one-dimensional pore system even by its small quantity. Nevertheless, the relatively high CO_2 volume measured at saturation with the crystals synthesized from V_2O_5 indicates the high porosity of this compound (Fig. S2).

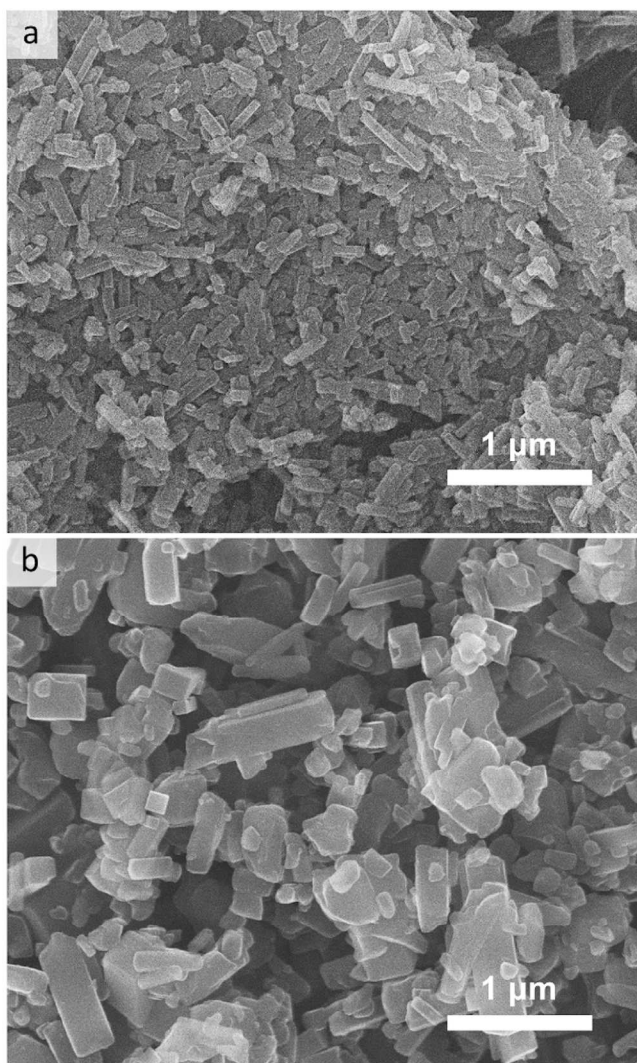


Fig. 6 FE-SEM micrographs of the $[\text{V}(\text{O})\text{ndc}]_n$ crystals synthesized from V_2O_5 powder (a) and of $[\text{V}(\text{O})\text{ndc}]_n$ synthesized from VCl_3 (b).

Importantly, the addition of ascorbic acid to the reaction medium was the key for the successful conversion of V_2O_5 into $[\text{V}(\text{OH})\text{ndc}]_n$. Ascorbic acid plays a critical role in the metal oxide dissolution. Indeed, V_2O_5 used as metal source was systematically recovered at the end of reactions performed without ascorbic acid. Ascorbic acid is thus most likely involved in the ligand-assisted dissolution, a phenomenon that is known to promote the dissolution of minerals in the presence of organic chelating molecules in natural environment.¹⁹ In the case of metal oxides made of redox active ions, such as iron or chromium oxides, two types of ligand-assisted dissolution mechanism were identified: a non-reductive and a reductive processes. Ligand-assisted dissolution occurring through the non-reductive process relies on the adsorption of chelating ligands on metal ions accessible on the mineral surface that weakens the metal-oxygen bonds and results in the desorption of the surface complex. In the reductive pathway, the enhancement of the metal-oxygen lability (and the subsequent surface complex desorption) is induced by the reduction of the metal ions through an electron transfer from the complex to the metal center. While reductive dissolution process was clearly identified in the case of iron²⁰ and chromium oxides,²¹ reports about V_2O_5 ligand-assisted

dissolution evoking a reductive dissolution process are scarce. So far, the dissolution of V_2O_5 in aqueous solution of oxalic acid at 25°C was rather shown to be ruled by a non-reductive ligand-assisted mechanism.²² However, the formation of the as-synthesized $[\text{V}^{\text{III}}(\text{OH})\text{ndc}]_n$ for which the oxidation state of the vanadium is known to be (III) (or a mix of (III) and (IV) as mentioned before) clearly indicates the reduction of the vanadium centers before the formation of the PCP framework. The ability of ascorbic acid to reduce V^{V} into V^{IV} through the formation of an ascorbate-vanadate complex is well-known.²³ The stoichiometry of the reduction was determined to be $\text{H}_2\text{A} + 2\text{V}^{5+} \rightarrow \text{A} + 2\text{V}^{4+} + 2\text{H}^+$ (where H_2A is ascorbic acid and A is the corresponding oxidation product), a one-electron transfer within the complex being the most plausible reduction mechanism. It has also been shown that, given sufficient time, ascorbic acid can also reduce V^{IV} into V^{II} with the formation of V^{III} intermediate species.²⁴ Thus, in our case, a reductive dissolution mechanism should not be discarded, especially because high temperatures, such as the one set in our study (180°C), is known to promote both reductive and non-reductive dissolution process.^{20,25} The clear distinction between a pure reductive dissolution and a non-reductive dissolute-ion followed by the subsequent homogeneous reduction of the dissolved vanadium species in the bulk solution would require the detailed investigation of V_2O_5 dissolution and reduction kinetics as well as speciation, which is beyond the scope of this work.

The reduction of dissolving vanadium species to the proper oxidation state by ascorbic acid is also expected to make the formation of the $[\text{V}^{\text{III}}(\text{OH})\text{ndc}]_n$ framework possible. Indeed, similarly to the members of the isostructural framework family of the general formula $[\text{M}^{\text{III}}(\text{OH})\text{L}]_n$ (where M is Al, Fe, Cr, Ga, Sc or In and L is a 1,4-benzenedicarboxylate derivative), $[\text{V}(\text{OH})\text{ndc}]_n$ framework is built through the assembly of trivalent vanadium cations in a regular octahedra coordination environment. While $[\text{V}^{\text{IV}}(\text{O})\text{ndc}]_n$ can be obtained through an oxidation step during which $[\text{V}^{\text{III}}(\text{OH})]^{2+}$ are converted into $[\text{V}^{\text{IV}}(\text{O})]^{2+}$ with the maintenance of the neutrality of the resulting framework, the synthesis of the same framework directly from V^{IV} and V^{V} as metal source is unlikely. Indeed, in aqueous solution, V^{IV} and V^{V} precursors form distorted octahedron (VO_6) consisting of a short vanadyl bond ($\text{V}=\text{O}$) associated to a long V-O bond in the opposite direction.²⁶ In this configuration, the non-bonding nature of the $\text{V}=\text{O}$ double bond commonly results in the formation of layered compounds, e.g. the layered V_2O_5 .^{9,26} Such precursors may not permit the construction of the infinite chains made of corner sharing vanadium regular octahedron commonly encountered within $[\text{M}^{\text{III}}(\text{OH})\text{L}]_n$ compounds (Fig. 1). On the other hand, the reduction of V_2O_5 by ascorbic acid as reducing agent enables to obtain the oxidation state V^{III} whose regular octahedral coordination environment allows the formation of the $[\text{V}^{\text{III}}(\text{OH})\text{ndc}]_n$ framework.

Importantly, we also verified the generalizability of this new PCP synthesis route with the preparation of $[\text{V}(\text{OH})\text{bdc}]_n$, where bdc is the 1,4-benzenedicarboxylate ligand, using V_2O_5 powder as metal source (Fig. S3 and S4).

Replication of V_2O_5 macrostructures

After demonstrating the synthesis of $[\text{V}^{\text{III}}(\text{OH})\text{ndc}]_n$ (and $[\text{V}^{\text{IV}}(\text{O})\text{ndc}]_n$ after activation) from V_2O_5 , we established the coordination replication process of V_2O_5 patterns and nanofibers into the analogous PCP polycrystalline structures. The vanadium oxide two-dimensional pattern was prepared by

using 10 μm PS beads assemblies as hard templates. The negative structure of the PS bead assembly made of a vanadium oxide phase was obtained after complete removal of the PS beads (Fig. 7a).

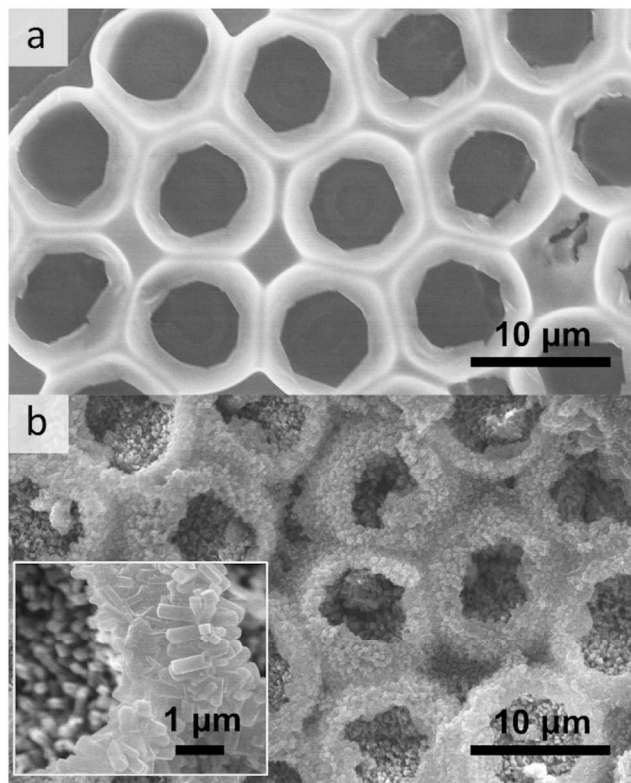


Fig. 7 FE-SEM micrographs of (a) the V_2O_5 pattern and (b) the $[\text{V}(\text{OH})\text{ndc}]_n$ pattern obtained after coordination replication. The SEM image in inset is a high magnification view of the PCP pattern.

The two strong bands observed at 1026 cm^{-1} and 837 cm^{-1} in the attenuated total reflectance mode (ATR) FT-IR spectra of the resulting pattern unambiguously indicates the formation of the V_2O_5 phase (Fig. S5). The presence of the intense and relatively broad peak observed at $2\theta = 8.4^\circ$ in the XRD pattern of the same sample suggests that the patterns are made of a hydrous $\text{V}_2\text{O}_5 \cdot n\text{H}_2\text{O}$ phase with a layered structure composed of V_2O_5 sheets in between which water molecules are intercalated (Fig. 8).²⁷ Indeed, this 8.4° peak can be assigned to the (001) diffraction, which is related to the V_2O_5 layer stacking along the direction perpendicular to the layer plane. The others broad diffraction peaks observed above $2\theta = 10^\circ$ could not be attributed.

The $\text{V}_2\text{O}_5 \cdot n\text{H}_2\text{O}$ pattern was then converted into a $[\text{V}(\text{OH})\text{ndc}]_n$ polycrystalline structure with an identical morphology during a microwave treatment at 180°C for 1 s, in the presence of an aqueous solution of H_2ndc ligands. FE-SEM analysis of the patterns obtained after microwave treatment clearly demonstrated the transformation of the smooth $\text{V}_2\text{O}_5 \cdot n\text{H}_2\text{O}$ surface into an assembly of well-intergrown cuboid crystals (Fig. 7b). Formation of the $[\text{V}(\text{OH})\text{ndc}]_n$ crystals was confirmed by both XRD and IR analyses (Figs. 8b and S5b, respectively). Total consumption of the layered $\text{V}_2\text{O}_5 \cdot n\text{H}_2\text{O}$ parent phase is indicated by the total vanishing of the $d(001)$ peak at $2\theta = 8.4^\circ$.

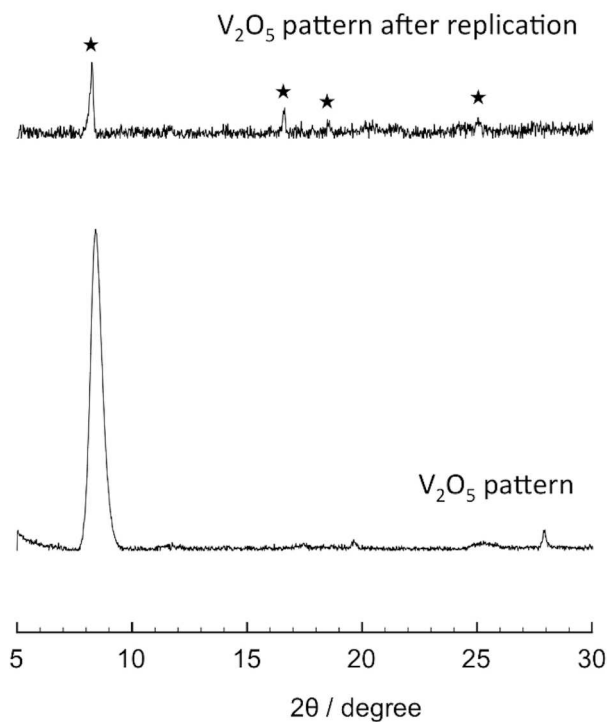


Fig. 8 PXR D pattern of the V_2O_5 pattern before and after replication into $[\text{V}(\text{OH})\text{ndc}]_n$ polycrystalline structure. The stars highlight the diffraction peaks corresponding to $[\text{V}(\text{OH})\text{ndc}]_n$.

Noteworthy, the success of the coordination replication procedure for the synthesis of $[\text{V}(\text{OH})\text{ndc}]_n$ crystal pattern relied on some modifications of the synthesis procedure of $[\text{V}(\text{OH})\text{ndc}]_n$ using V_2O_5 powder. First, the coordination replication was performed with an amorphous V_2O_5 parent phase instead of a crystalline phase. Indeed, the crystalline V_2O_5 pattern obtained after a heating treatment at 320°C for 10 h (Fig. S6) was not appropriate since it was systematically washed away during the microwave treatment, probably due to the lack of strong enough interactions between the V_2O_5 crystals and the glass substrate (data not shown). Second, the reaction time was reduced from 10 min to 1 s in order to preserve the macroscopic morphology of the V_2O_5 pattern. Longer reaction times resulted in the complete removal of the pattern from the substrate (data not shown). Third, a PEO layer was coated on the top of the V_2O_5 pattern prior to the microwave treatment. This step was shown to be critical to preserve the morphology of the parent vanadium oxide phase during the dissolution replication process. Indeed, during this process, particular care have to be taken to maintain the dissolution kinetics of the metal oxide sacrificial phase lower than the kinetic of the PCP crystallization in order to guarantee that the PCP nucleation occurs at the vicinity of the dissolution front.²⁸ In water and under mild acidic conditions, PEO is known to form weak coordination complexes similar to crown ethers with various metal cations including vanadium.²⁹ Here, we assume that the PEO coating acts as a trap, which slow down both V_2O_5 dissolution and the diffusion of the ionic vanadium species at the solid-liquid interface.

Conclusion

In conclusion, we synthesized a polycrystalline macrostructure with a designed morphology made of intergrown $[V(OH)ndc]_n$ crystals by a reductive coordination replication process. Utilization of V_2O_5 as metal source requires the addition of ascorbic acid as reducing agent in order to generate the V^{III} species at the origin of the $[V(OH)ndc]_n$ inorganic backbone. Because of the versatility of the sol-gel and solid-state processes applied to vanadium oxide chemistry, the general process reported in this contribution affords a powerful mean for the preparation of a variety of new functional PCP-based macrostructures, such as heterogeneous catalysts with hierarchical porosity.

Acknowledgements

This work was supported by a Grant-in-Aid for Scientific Research (No. 24108720 for Innovative Areas "Coordination Programming" Area 2107, and No. 25708010 for Wakate A) from MEXT, Japan. iCeMS is supported by the World Premier International Research Initiative (WPI), MEXT, Japan. The authors thank CeMI for assistance with electron microscopy.

Notes and references

^a Institute for Integrated Cell-Material Sciences (WPI-iCeMS), Kyoto University, Yoshida, Sakyo-ku, Kyoto 606-8501, Japan.

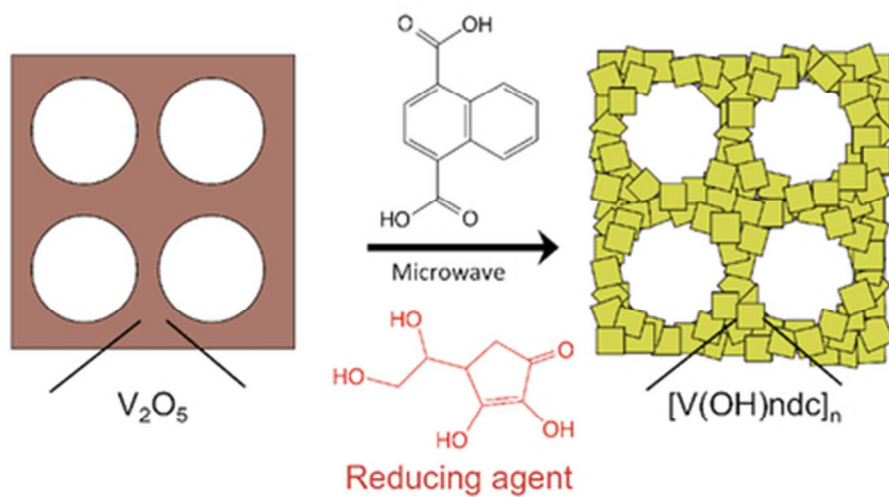
^b Department of Synthetic Chemistry and Biological Chemistry, Graduate School of Engineering, Kyoto University, Katsura, Nishikyo-ku, Kyoto 615-8510, Japan.

Electronic Supplementary Information (ESI) available: the TG analysis of the as-synthesized $[V(OH)ndc]_n$ synthesized from V_2O_5 powder and of the as-synthesized $[V(OH)ndc]_n$ synthesized from VCl_3 , CO_2 adsorption and desorption isotherms of $[V(O)ndc]_n$ synthesized from V_2O_5 powder and of $[V(O)ndc]_n$ synthesized from VCl_3 , the PXRD patterns of the activated $[V(O)bdc]_n$, the PXRD pattern and IR spectra of the activated $[V(O)bdc]_n$ obtained from VCl_3 and from V_2O_5 , the PXRD pattern and FT-IR spectra of the V_2O_5 pattern before and after conversion into $[V(OH)bdc]_n$, the FT-IR spectra of the V_2O_5 pattern before replication and after replication into $[V(OH)ndc]_n$ structure and a FE-SEM image of the crystalline V_2O_5 pattern.

See DOI: 10.1039/c000000x/

- (a) O. M. Yaghi, M. O'Keefe, N. W. Ockwing, H. K. Chae, M. Eddaoudi and J. Kim, *Nature*, 2003, **423**, 705; (b) S. Kitagawa, R. Kitaura and S. Noro, *Angew. Chem., Int. Ed.*, 2004, **43**, 2334; (c) G. Férey, *Chem. Soc. Rev.*, 2008, **37**, 191.
- (a) P. Van Der Voort, K. Leus, Y.-Y. Liu, M. Vandichel, V. Van Speybroeck, M. Waroquier and S. Biswas, *New J. Chem.*, in press. DOI: 10.1039/c3nj01130e; (b) Y.-Y. Liu, S. Couck, M. Vandichel, M. Grzywa, K. Leus, S. Biswas, D. Volkmer, J. Gascon, F. Kapteijn, J. F. M. Denayer, M. Waroquier, V. Van Speybroeck and P. Van Der Voort, *Inorg. Chem.*, 2013, **52**, 113; (c) K. Leus, I. Muylaert, M. Vandichel, G. B. Marin, M. Waroquier, V. Van Speybroeck and P. Van Der Voort, *Chem. Commun.*, 2010, **46**, 5085.
- (a) S. Furukawa, J. Reboul, S. Diring, K. Sumida, and S. Kitagawa, *Chem. Soc. Rev.* 2014, **43**, 5700.; (b) O. Shekhah, J. Liu, R. A. Fischer and C. Wöll, *Chem. Soc. Rev.*, 2011, **40**, 1081; (c) Y.-N. Wu, F. Li, W. Zhu, J. Cui, C. A. Tao, C. Lin, P. M. Hannam and G. Li, *Angew. Chem. Int. Ed.*, 2011, **50**, 12518; (d) P. Falcaro, R. Ricco, C. M. Doherty, K. Liang, A. J. Hill, and M. J. Styles, *Chem. Soc. Rev.* 2014, **43**, 5513.
- J. Reboul, S. Furukawa, N. Horike, M. Tsotsalas, K. Hirai, H. Uehara, M. Kondo, N. Louvain, O. Sakata and S. Kitagawa, *Nat. Mater.*, 2012, **11**, 717.
- Handbook of Sol-Gel Science and Technology. Processing, Characterization and applications, ed. by Sumio Sakka, Springer, New York, 2005.
- K. Khaletskaia, J. Reboul, M. Keilikhov, M. Nakahama, S. Diring, M. Tsujimoto, S. Isoda, F. Kim, K. Kamei, R. A. Fischer, S. Kitagawa and S. Furukawa, *J. Am. Chem. Soc.*, 2013, **135**, 10998.
- (a) W. Zhan, Q. Kuang, J. Zhou, X. Kong, Z. Xie and L. Zheng, *J. Am. Chem. Soc.*, 2013, **135**, 1926; (b) I. Stassen, N. Campagnol, J. Franssaer, P. Vereecken, D. E. De Vos and R. Ameloot, *CrystEngComm*, 2013, **15**, 9308.
- Y. Liu, W. Zhang, S. Li, C. Cui, J. Wu, H. Chen and F. Huo, *Chem. Mater.*, 2014, **26**, 1119.
- J. Livage, *Solid State Ionics*, 1996, **86**, 935.
- (a) J. Livage, G. Guzman, F. Beteille and P. Davidson, *J. Sol-Gel Sci. Technol.*, 1997, **8**, 857; (b) Y. Wang, K. Takahashi, K. Lee and G. Cao, *Adv. Funct. Mater.*, 2006, **16**, 1133; (c) L. Mai, L. Xu, C. Han, X. Xu, Y. Luo, S. Zhao and Y. Zhao, *Nano Lett.*, 2010, **10**, 4750; (d) L. Li, U. Steiner and S. Mahajan, *J. Mater. Chem.*, 2010, **20**, 7131.
- M. Nakahama, J. Reboul, K.-I. Kamei, S. Kitagawa and S. Furukawa, *Chem. Lett.*, 2014, **43**, 1052.
- (a) O. Kozachuk, M. Meilikhov, K. Yusenko, A. Schneemann, B. Jee, A. V. Kuttathayil, M. Bertmer, C. Sternemann, A. Pöpl and R. A. Fischer, *Eur. J. Inorg. Chem.*, 2013, **26**, 4546; (b) K. Barthelet, J. Marrot, D. Riou and G. Férey, *Angew. Chem.*, 2002, **41**, 281.
- A. Comotti, S. Bracco, P. Sozzani, S. Horike, R. Matsuda, J. Chen, M. Takata, Y. Kubota and S. Kitagawa, *J. Am. Chem. Soc.*, 2008, **130**, 13664.
- H. Leclerc, T. Devic, S. Devautour-Vinot, P. Bazin, N. Audebrand, G. Férey, M. Daturi, A. Vimont and G. Clet, *J. Phys. Chem. C*, 2011, **115**, 19828.
- Z. Ni and R. I. Masel, *J. Am. Chem. Soc.*, 2006, **128**, 12394.
- L. Hamon, H. Leclerc, A. Ghoufi, L. Oliviero, A. Travert, J.-C. Lavalley, T. Devic, C. Serre, G. Férey, G. De Weireld, A. Vimont and G. Maurin, *J. Phys. Chem. C*, 2011, **115**, 2047.
- (a) Y.-Y. Liu, K. Leus, M. Grzywa, D. Weinberger, K. Strubbe, H. Vrielinck, R. Van Deun, D. Volkmer, V. Van Speybroeck and P. Van Der Voort, *Eur. J. Inorg. Chem.*, 2012, 2819; (b) A. Centrone, T. Harada, S. Speakman and T. A. Hatton, *Small*, 2010, **6**, 1598.
- I. L. Botto, M. B. Vassallo, E. J. Baran and G. Minelli, *Mater. Chem. Phys.*, 1997, **50**, 267.
- W. Stumm and R. Wollast, *Rev. Geophys.*, 1990, **28**, 53.
- D. Panias, M. Taxiarchou, I. Paspaliaris and A. Kontopoulos, *Hydrometallurgy*, 1996, **42**, 257.
- L. A. García Rodenas, A. M. Iglesias, A. D. Weisz, P. J. Morando and M. A. Blesa, *Inorg. Chem.*, 1997, **36**, 6423.
- V. I. E. Bruyère, P. J. Morando and M. A. Blesa, *J. Colloid Interface Sci.*, 1999, **209**, 207.

- 23 (a) K. Kustin and D. L. Toppen, *Inorg. Chem.*, 1973, **12**, 1404; (b) P. C. Wilkins, M. D. Johnson, A. A. Holder and D. C. Crans, *Inorg. Chem.*, 2006, **45**, 1471.
- 24 M. M. Taqui Khan and A. E. Martell, *J. Am. Chem. Soc.*, 1968, **90**, 6011.
- 25 R. M. Sella and W. J. Williams, *Faraday Discuss. Chem. Soc.*, 1984, **77**, 265.
- 26 A. A. Belik, A. V. Mironov, R. V. Shpanchenko and E. Takayama-Muromachi, *Acta Crystallogr., Sect. C*, 2007, **63**, 37.
- 27 V. Petkov, P. N. Trikalitis, E. S. Bozin, S. J. L. Billinge, T. Vogt and M. G. Kanatzidis, *J. Am. Chem. Soc.*, 2002, **124**, 10157.
- 28 A. Putnis, *Rev. Miner. Geochem.*, 2009, **70**, 87.
- 29 K. G. Vassilev, R. Stamenova and C. B. Tsvetanov, *Comptes rendus de l'académie bulgare des Sciences*, 2000, **53**, 51.



39x22mm (300 x 300 DPI)